Austrian Journal of Earth Sciences | Volume 107/2 | 112 - 130 | Vienna | 2014

Sedimentation of the Paleogene Liushagang Formation and the response to regional tectonics in the Fushan Sag, Beibuwan Basin, South China Sea

Siding JIN[1)2)*)], Hua WANG[1)], Haiyang CAO[1)], Si CHEN[1)], Zhengliang LIN[3)], Jianghao YU[4)] & Songqi PAN[5)6)]

[1)] Key Laboratory of Tectonics and Petroleum Resources, China University of Geosciences, Wuhan 430074, China;

[2)] Department of Geodynamics and Sedimentology, University of Vienna, Althanstrasse 14, 1090 Wien, Austria;

[3)] Sinopec Geophysical Research Institute, Nanjing 210014, China;

[4)] Hubei Institute of Geological Survey, Wuhan 430034, China;

[5)] School of Earth and Space Sciences, Peking University, Beijing 100871, China;

[6)] Petro China Research Institute of Petroleum Exploration & Development, Beijing 100083, China;

[*)] Corresponding author, jinsiding@gmail.com

KEYWORDS

Liushagang Formation
Tectonic evolution
Beibuwan Basin
Sediment infill
Fushan Sag

Abstract

The sediments of the Liushagang Formation in the Fushan Sag (Paleogene of the South China Sea) are preserved in a variety of structural settings and are described in a sequence stratigraphic framework. This paper presents the control of the sedimentary infill by the tectonic evolution of the Fushan Sag based on the integration of available cores data, corresponding well-logs interpretation, seismic interpretations, sedimentary distribution and spatial evolution analysis, fault activity rate calculation and paleogeographic reconstructions.

Three third order sequences SQEls3, SQEls2 and SQEls1 are identified within the Eocene Liushagang Formation by sequence boundaries and maximum flooding surfaces based on seismic interpretations. Three sedimentary systems are identified: (1) a fan delta system, (2) braided river delta system and (3) a lake system inclduing turbidite deposits. The sandstone proportion in the three delta areas decreased from SQEls3 to SQEls2, which indicates a continuously transgression, showing the transition from proximal to distal sites in most wells, and an obvious decrease of fan delta sizes. The northeast-southwest striking faults control the lakeward distributions of delta fronts and turbidite fans.

Tectonism is the main controlling factor for the sedimentary infill of the Fushan Sag. Syn-rifting tectonic subsidence, controls the spatial-temporal sediment distribution. The more active western part of the Lingao Fault has an important influence on the northeastward migration of depocenters in the Liushagang Formation. Tectonic activity along the eastern boundary fault in the Fushan Sag increased first and then decreased, which influences the fan delta system in the Bailian sub-sag. The tectonic activity along the Meitai Fault obviously increased since Els2, which controls the turbidite system in Els2, the delta plain and delta front distributions in Els1. The topography developed continuously from Els3 to Els1, and the diminished subsidence indicates the dominant geological process varying from intense fault rifting in an early period to relatively gentle and overall subsidence in a later period during the Paleogene.

1. Introduction

Tectonic activity is an important control on sedimentary systems among the interaction of several factors, such as sea level change, sediment supply, and climate changes, both in marine and lacustrine basins (e.g., Lin et al., 2001, 2005; Strecker et al., 1999). Synsedimentary tectonism may be the major factor controlling sequence architectures and sedimentary patterns, as it directly alters accommodation, changes depositional base level and influences the distribution of source areas in tectonically active continental rift basins (e.g. Devlin et al., 1993; Williams, 1993). With a close relation to the tectonic activities including fault activity, subsidence rate and paleogeomorphology, the sedimentary infill and spatial distribution reflect the control of dynamic tectonic movements and episodic sedimentations in a sequence stratigraphic framework in the Paleogene of the Fushan Sag, Beibuwan Basin, South China Sea (e.g. Wang et al., 2007; Liao et al., 2012).

Regarding the Fushan Sag, previous studies focused on the sequence stratigraphy, infill architecture (Ma et al., 2012; Sun et al. 2013), reservoir properties (Liu et al., 2013; Song et al., 2000), structural features (Liu et al., 2013a, b; Luo and Pang, 2008;), and petroleum systems (Zhang et al. 2012; Ding et al., 2003; Li et al., 2007, 2008). Sedimentary systems have been studied in detail (Liu et al., 2003a, b; Liu and Gao, 2000; He and Gao, 2006; Li et al., 2010,) as well as the regional tectonic evolution (Yu et al., 2012; Lin, 2009). However, the sedimentary analysis should take into consideration not only syn-sedimentary structures in spatial but also the tectonic evolution in a temporal framework. There are few publications that link the sedimentation to the tectonic evolution, especially of the Paleogene Liushagang Formation. Thus, this paper is primarily intended to achieve a better and comprehensive understanding of sediment infill features and their responses to the tectonic evolution within a chronostratigraphic sequence stratigraphic framework.

In order to resolve the problems, a variety of existing data from facies analysis of available cores, interpretation of corresponding well-logs (supported by PetroChina Fushan Oilfield Company) is used, combined with seismic interpretation and sequence stratigraphy. The main goals of this paper are to document sediment infill features and their responses to the tectonic evolution through the evaluation of tectonic activity, basin subsidence, paleogeomorphology, and detailed research of longitudinal sedimentary evolution with the superimposition of paleogeomorphology that is based on the original strata recovery data.

2. Geological Setting

2.1 Regional geologic background of the Beibuwan Basin

The Beibuwan Basin is a Mesozoic-Cenozoic intraplate rift basin in the northern continental shelf of the South China Sea, located in the southeast margin of Eurasian plate, adjacent to the India-Australia plate and the Pacific plate (Fig. 1a). It is a petroliferous basin located northeast of the Yinggehai Basin, and northwest of the Qiongdongnan Basin, with an area of 350,000 km^2 (Zhang and Su, 1986; Kang et al., 1994; Du, 1997; Wei et al., 2008; Li et al, 2012; Zhu et al., 2004; Fang, 1983; Liu et al, 2008). Lithospheric thinning processes and extension in the northern continental margin of the South China Sea formed several continental marginal basins since Late Cretaceous, including the Zhujiangkou Basin, the Yinggehai Basin and the Qiongdongnan Basin (Shi et al., 2000; Tian and Wang, 1985). The size of those rift basins increases from NW to SE, which reflects a dynamic processes of lithospheric thinning and crustal extension from continental crust to finally oceanic crust (Yao and Hayes, 1998).

From north to south, the Beibuwan Basin is divided into three first-order structural units (Li et al, 2012; Jiang, 2007): the Northern Depression, the Qixi Uplift and the Southern Depression. These units can be further subdivided into sub-units: the Changhua half graben sub-basin, the Haizhong rift sub-basin, the Weixinan half graben sub-basin, the Wushi half graben sub-basin, the Haitoubei half graben sub-basin, the Maichen rift sub-basin, the Jinghe rift sub-basin, and the Fushan Sag (Fig. 2). These sub-basins developed along a variety of normal faults with NE, NEE or NW trends.

2.2 Geologic background of the Fushan Sag

The Fushan Sag is located at the southern margin of the Beibuwan Basin (Fig. 1a), with a total area of about 2,920 km^2 and a maximum Cenozoic depositional thickness of about 9,000 m (Shi et al., 2007; Zhang et al., 2012). Three positive geomorphic units limit the Fushan Sag including the western Lingao Uplift, eastern Yunlong Uplift and the southern Hainan Basement. All highs provided source areas for sediments of

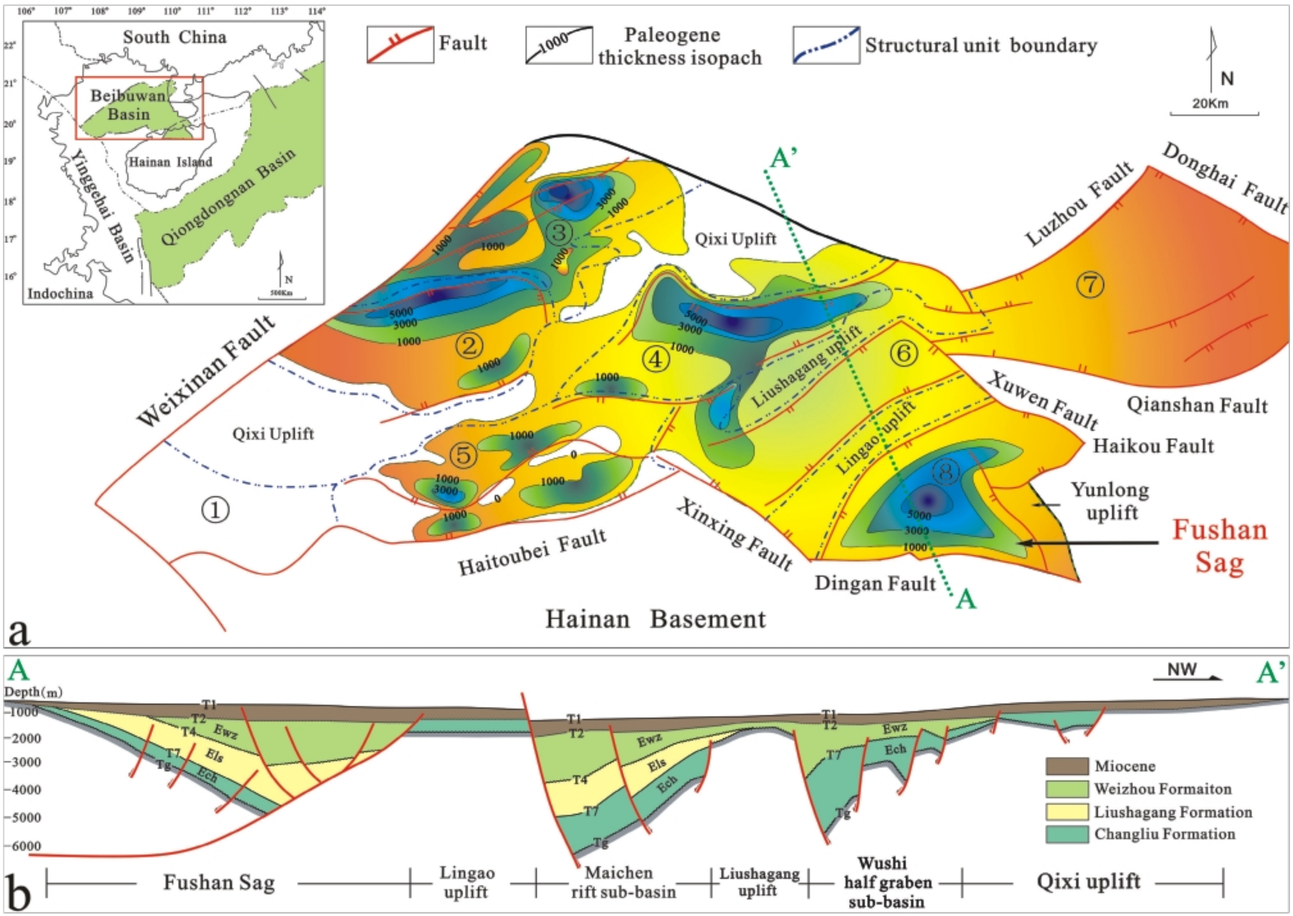

Figure 1: Geological outline map of the Beibuwan Basin (Zhu et al., 2004; Lu and Wang, 2007; Kang et al., 2007; Li et al., 2012). (a) The Beibuwan Basin contains eight sub-basins: (1) Changhua half graben sub-basin, (2) Haizhong rift sub-basin, (3) Weixinan half graben sub-basin, (4) Wushi half graben sub-basin, (5) Haitoubei half graben sub-basin, (6) Maichenrift sub-basin, (7) Jinghe rift sub-basin, and (8) Fushan Depression. (b) The NW-SE schematic structure section crosses three sub-basin in the east of Beibuwan Basin.

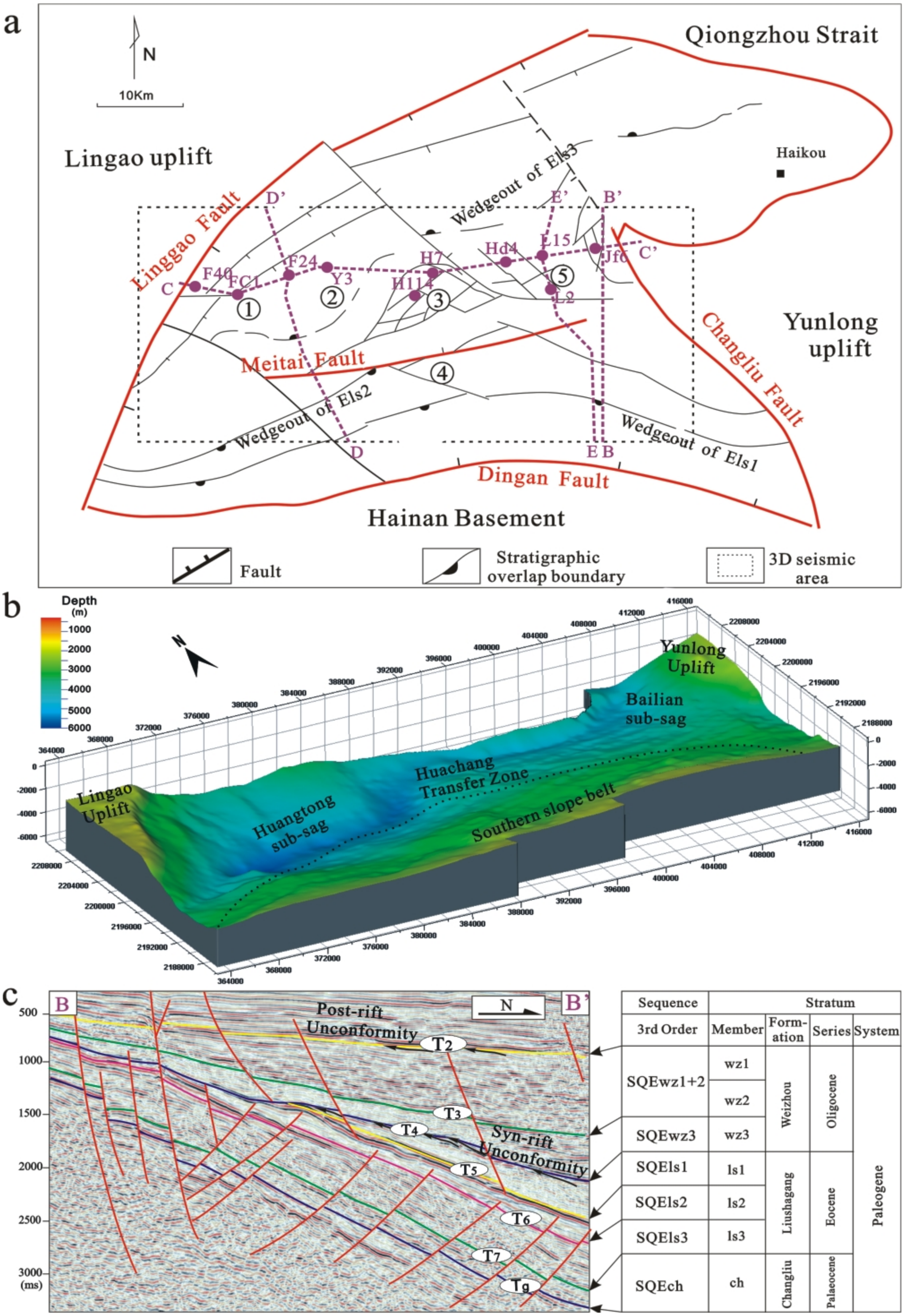

Sequence	Stratum			
3rd Order	Member	Form-ation	Series	System
SQEwz1+2	wz1	Weizhou	Oligocene	Paleogene
	wz2			
SQEwz3	wz3			
SQEls1	ls1	Liushagang	Eocene	
SQEls2	ls2			
SQEls3	ls3			
SQEch	ch	Changliu	Palaeocene	

Figure 2: (a) Outline map of the Fushan Sag with five secondary tectonic units. (1) Bohou step-fault zone; (2) Huangtong sub-sag; (3) Huachang transfer zone; (4) Southern slope belt; (5) Bailian Sub-sag. (b) Basement topography of the Fushan Sag. (c) Sequence stratigraphic framework of the Paleogene in Fushan Sag. wz1+2 = Member 1 and member 2 of the Weizhou Formation; wz3 = Member 3 of the Weizhou Formation; ls1 = Member 1 of the Liushagang Formation; ls2 = Member 2 of the Liushagang Formation; ls3 = Member 3 of the Liushagang Formation; ch = Changliu Formation. See dotted line BB' in Fig. 2A to locate this survey line.

the Fushan Sag and were controlled by boundary faults such as the Lingao Fault in the northwest, the Changliu Fault in the northeast and the Dingan Fault in the south. All these faults developed since the rifting stage in Paleogene, giving way to a triangle-shape of the Fushan Sag. The Sag forms a half-graben faulted in the south and overstepping in the north. Five secondary structural units exist: (1) the Bohou step-fault zone, (2) the Huangtong sub-sag, (3) the Huachang transfer zone, (4) the southern slope belt and (5) Bailian sub-sag (Fig. 2a, b). Previous researches (Liu et al, 2012, 2013; Lin, 2011; Yu et al, 2004) interpreted the Fushan Sag as an east-west trending transfer zone (Huachang transfer zone) which separated two extensional systems (Huangtong and Bailian sub-sags, see Fig. 7a). The Paleogene strata in the Fushan Sag comprises three formations: the Changliu (Ech), Liushagang (Els), and Weizhou (Ewz) Formations (Fig. 2c) (Liu et al., 2003 a, b; Li et al, 2007; He and Gao, 2006).

Like other basins in the South China Sea, the Fushan Sag underwent four major tectonic episodes from the Mesozoic to Neogene: (1) the Shenhu phase resulting in initial rifting during the Late Cretaceous, (2) the Zhuqiong phase as the main period of rifting during the early Paleogene, (3) the Nanhai phase was the transitional period from fault depression to sag during the late Paleogene, (4) stable subsidence occurred during the same period of the Dongsha phase in the Neogene (Fig. 3) (Gong, 1997; Qiu and Gong, 1999; Lin, 2011; Li et al., 2008). Therefore, three depositional hiatuses and three an-gular unconformities developed during the Paleogene in the Fushan Sag (Fig. 2c): (1) the unconformity (T5) between the Member 2 of Liushagang Formation (Els2) and the Member 1 of Liushagang Formation (Els1); (2) the unconformity (T4) between the Liushagang Formation (Els) and Weizhou Formation (Ewz) and (3) the unconformity (T2) between the Weizhou Formation (Ewz) and Neogene (N+Q).

According to the previous studies (Yu et al, 2013; Lin, 2011;

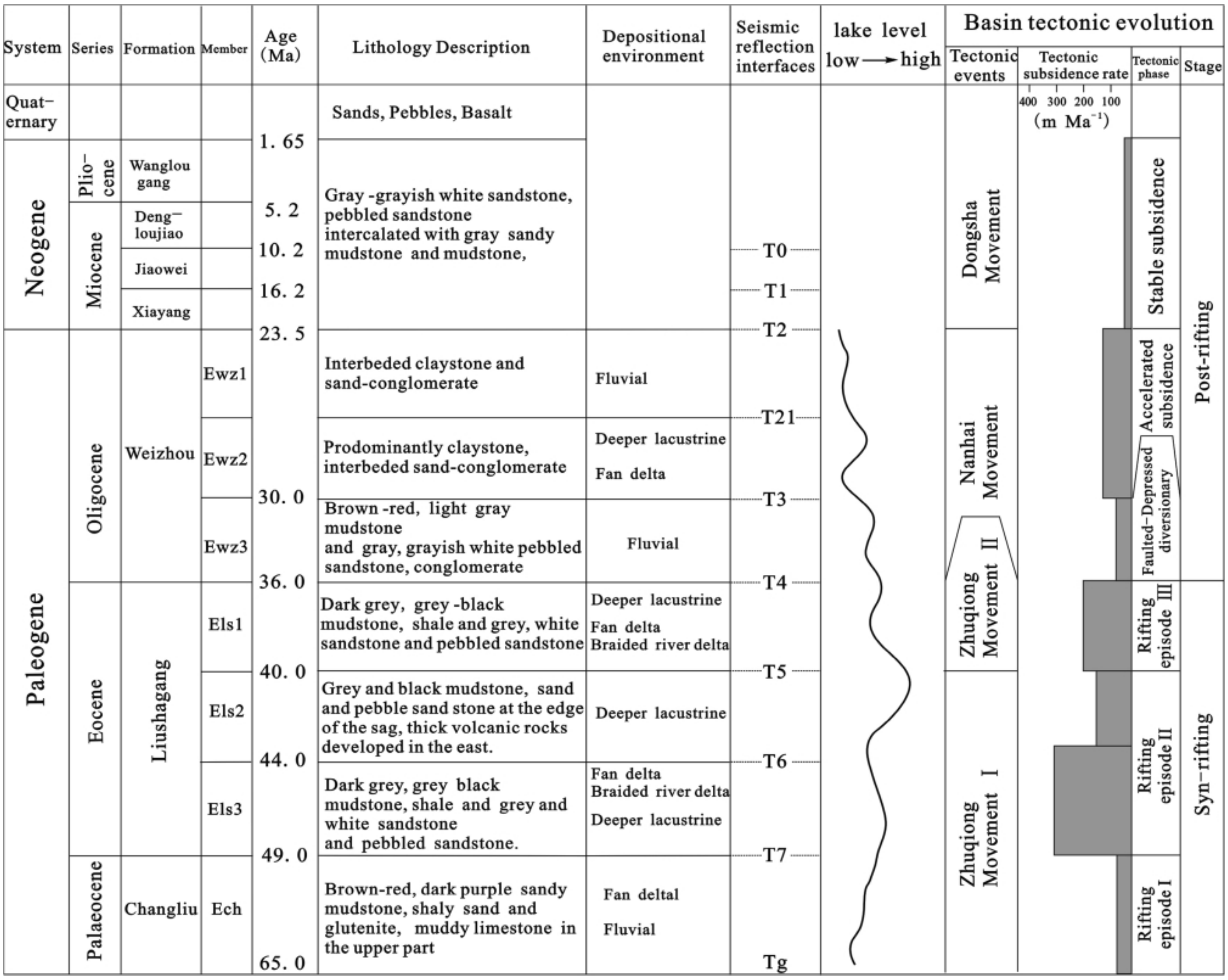

Figure 3: Sedimentary filling succession and tectonic evolution history in Paleogene in the Fushan Sag (Shi, 2007).

Ma et al., 2012; Zhu et al., 2008), the Fushan Sag is characterized by episodic subsidence during Paleogene to Neogene with T4 interpreted as syn-rifting and T2 as post-rifting unconformities (Fig.2b). At the beginning of the rifting stage in the Paleocene, the basin was mainly filled with alluvial and fluvial red sandstones of the Changliu Formation (Ech). Organic-rich mudstones were deposited in a series of well-developed lakes in the late rifting stage, and during the post-rifting stage, the basin was dominated by shallow lakes and swamps, leading to organic-rich mudstones with thin coal interbeds of the Weizhou Formation (Ewz3) (Li, 2008). The rifting stage can be further divided into three rifting periods: the rifting period I was the time during which the Changliu Formation (Ech) developed, the rifting period II (Fig. 3) was the time during which members 2 and 3 of the Liushagang Formation developed whereas Member 1 was deposited during rifting period III.

2.3 Petroleum Systems

The Fushan Sag, despite its relatively small size, has been a prolific producer of petroleum compared with other sub-basins of the Beibuwan Basin. To date, more than 30×104 t of oil and gas have been produced from Fushan Sag annually (Shi et al., 2007), six structural traps have been found including the Jinfeng, Chaoyang, Yongan, Huachang, Meitai trap and the Bailian trap. Among them, the Chaoyang trap is located in hanging wall of western boundary fault (Lingao Fault) and the Bailian trap lies in the hanging wall of eastern boundary fault (Changliu Fault). (Wang et al., 2010; Elena et al., 2007; Wu and Qi, 1999). The exceptional petroleum potential of the Fushan Sag is related to its complex fault systems, which contribute to the formation of fault block reservoirs, improve the quality of sandstone reservoirs, and control the maturation, migration, and the trapping of hydrocarbons.

3. Data and methods

The sequence stratigraphy framework is built using well logs, 3D seismic data, isopach maps, and geomorphology. Additionally, the method of the integration of point (wells), line (cross sections) and plane (planforms) information provides the framework for detecting and identifying the spatial and temporal evolution of the sedimentary fill (Chen et al., 2011, 2013; Shi et al., 2010).

1) Core data: three wells focused on specific areas of the Fushan Sag are presented for sedimentary environment analysis: Fc1 in the west, H114 in the center and L2 in the east (Figs. 4, 5 and 6, see Fig. 2a for the location of wells). We chose the typical cores in SQEls2 and SQEls1 because of the syn-depositional faults which mainly developed in Els2 and Els1. Based on grain size, lithofacies, sedimentary structures, and trace fossils, 76.22 meters of cores have been described and interpreted.
2) Seismic data: this study relies on 3D seismic profiles with an approximate area of 827km2 that was acquired by PetroChina Fushan Oilfield Company in 2006 (Fig. 2a). BB' and CC' seismic profiles are presented (Fig. 2c, Fig. 7a) to illustrate the internal stratigraphic architecture.
3) Inter-well correlation: 8 wells (F40, Fc1, F24, Y3, H7, Hd4, L15 and JF6, see Fig. 2a for the location of this profile) with lithology data, GR and RT log curves, were used in the lateral correlation and sedimentological analysis (Fig. 7a, b).
4) Time slices with facies distribution: By using multiple data of cores, well cuttings, log curves, seismic root mean square (RMS) amplitude, and statistics (sandstone/mudstone ratio and lithology percentage), time slices within the Liushagang Formation (Els) were defined (Fig. 8a, b, c). Based on 230 wells data (PetroChina Fushan Oilfield Company) including grain size, sandstone/mudstone ratio, and lithology percentage were used in delimiting the types of depositional systems, including the type of deposit system and the sediment source entry points in each member of Liushagang Formation of the Fushan Sag.
5) Fault activities: based on the seismic interpretations, we described the fault development of the Lingao Fault, Meitai Fault and Changliu Fault from 3D seismic, and interpreted fault throw data, using the geologic ages (Fig. 3) to calculate the fault's activities in each member of Liushagang Formation.
6) Temporal evolution data: After the 3D seismic data interpretation, the time domain horizons were transformed to depth domain horizons to build thickness isopach maps. According to the synthetic seismogram and seismic wave velocity, and detailed interpretation of the 3D seismic data, thicknesses of the third order sequences were reconstructed (Fig. 9a, b, c).
7) Subsidence history: older strata have been recovered by using the back stripping analysis (balance cross-section) technique (Fig. 10). Combining various strata adjustments (decompaction, paleobathymetry, lake-level changes etc.) (Chen et al., 2012; Chen et al., 2002; Liu and Jiang, 1995; Yan et al., 2003), the subsidence history of the Paleogene in the Fushan Sag has been calculated quantitatively by utilizing the EBM (Erosion recovery basin modeling) basin simulation system (Dahlstrom, 1969).
8) Superposition of paleotopography on the distribution of sedimentary facies: based on the total subsidence recovery data, the paleotopography has been reconstructed, which controlled the pattern and geometry of the sedimentary systems as a key to identify the development of sequences and sedimentary evolution in the filling stage in Fushan Sag. (Hentz, 1995; Deng et al., 2001; Escalona and Mann, 2010).

4. Results

4.1 Sedimentary systems of Liushagang Formation in the Fushan Sag as observed in cores

4.1.1 Well Fc1

Description

Well Fc1 is at the Chaoyang fault nose structure in the northwest of the Fushan Sag (Fig. 2a). The 26.57m of cores of

SQEls2 and SQEls1 from Well Fc1 are described below (Fig. 4).

From 3190.47 to 3186.27m cores (SQEls2) show brownish-black mudstones with massive structure, specular gloss, reflected a high organic content and high level of maturation. It contains poorly sorted sandstones with mud pebbles (Fig. 4K) at 3190.07-3189.17m. From 3130.67 to 3117.40m and 2071.10 to 2530.05 cores (SQEls1) show mudstones with high organic content, grey, cross-bedded sandstones (Fig. 4G), sandy con-

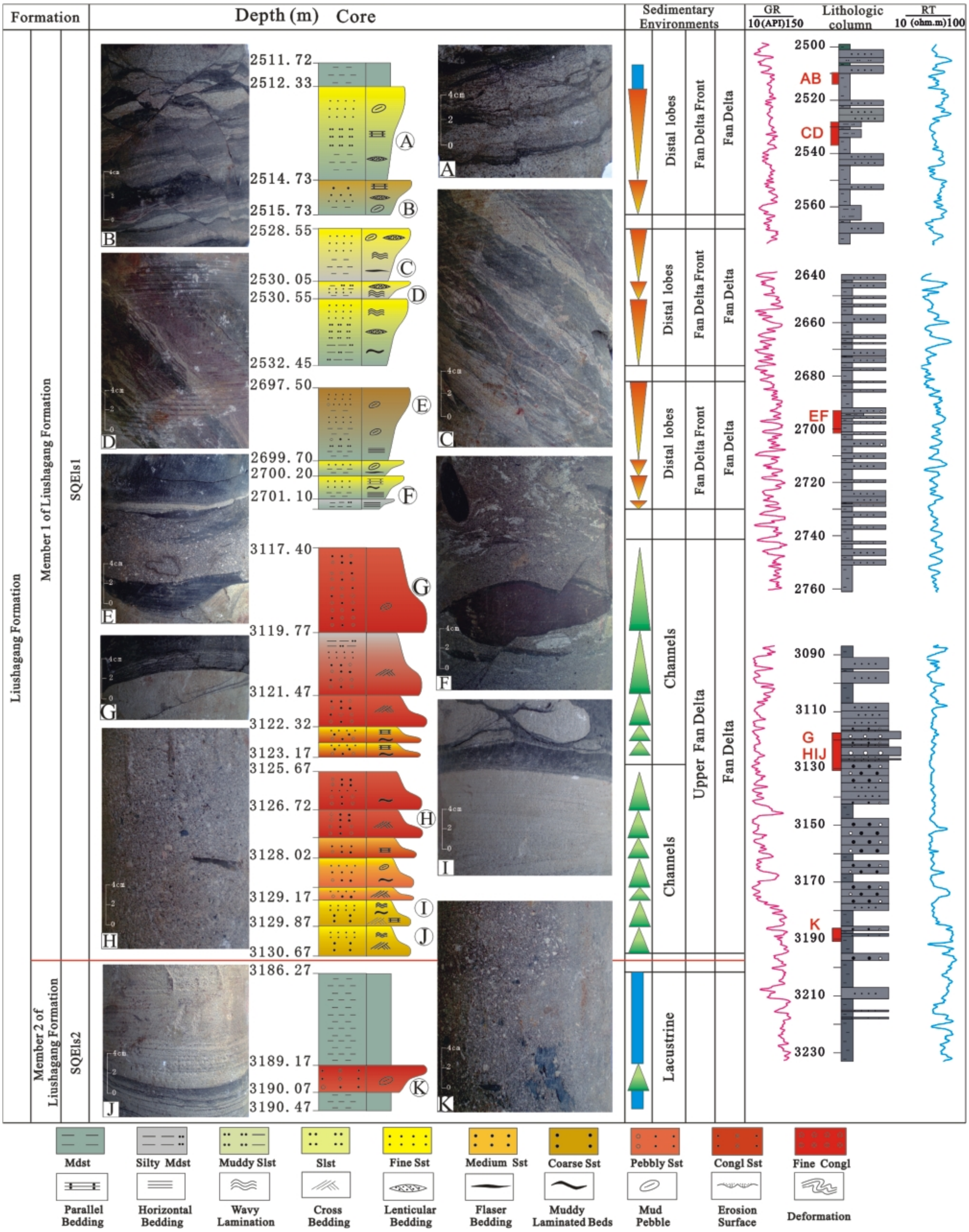

FIGURE 4: Macroscopic view of Well Fc1 cores. The 34.57 m cores in SQEls2 and SQEls1 occur from 3200 m to 2520 m.

glomerate, grey poorly sorted conglomerate sandstone (Fig. 4H), some places containing poorly sorted sandstones with mud pebbles (Fig. 4E), and sometimes displaying fining-upward sequences. Lenticular (Fig. 4B), flaser bedding, slumps,

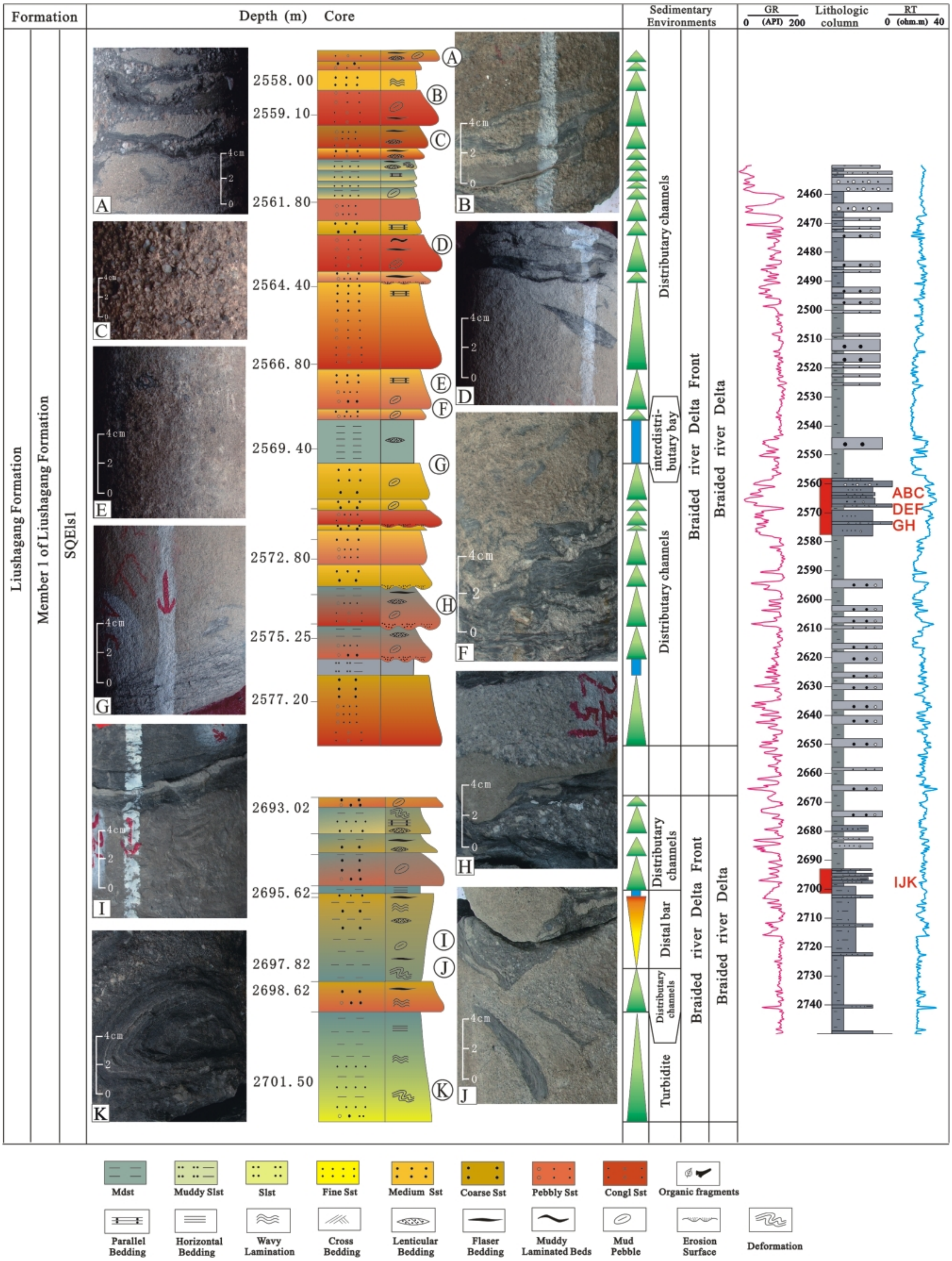

Figure 5: Macroscopic view of Well H114 cores. The 27.68 m cores in SQEls1 occur from 2710 m to 2550 m.

horizontal bedding (Fig. 4J), muddy laminated beds (Fig. 4D) and soft sedimentary deformation (Fig. 4I), brown nodules with minor fracture (Fig. 4F), and minor syn-sedimentary faults (Fig. 4C, A) are present.

Depositional environment interpretations:

The Well Fc1 core shows the SQEls1 and SQEls2 sequence. The cores of Els2 show that the main lithologic features are brownish-black mudstones. They also contain poorly sorted conglomerate sandstones. It is interpreted to be deposited in the lacustrine sedimentary environment including coarse fan deltas.

The core section of Els1 consists of two lithofacies associations: the lower part is dominated by grey conglomerate sandstones, coarse sandstones, and medium sandstones, as well as fine sandstones, the fining upward sequences are interpreted to be the channels of a fan delta; the upper part of the core section in Els1 developed several coarsening-upward sequences, and dominated by brownish-black and taupe mudstones, grey siltstones, and fine-medium sandstones which is interpreted as delta lobes at the fan delta front and slope. The GR log curve presents the high frequency serrated features.

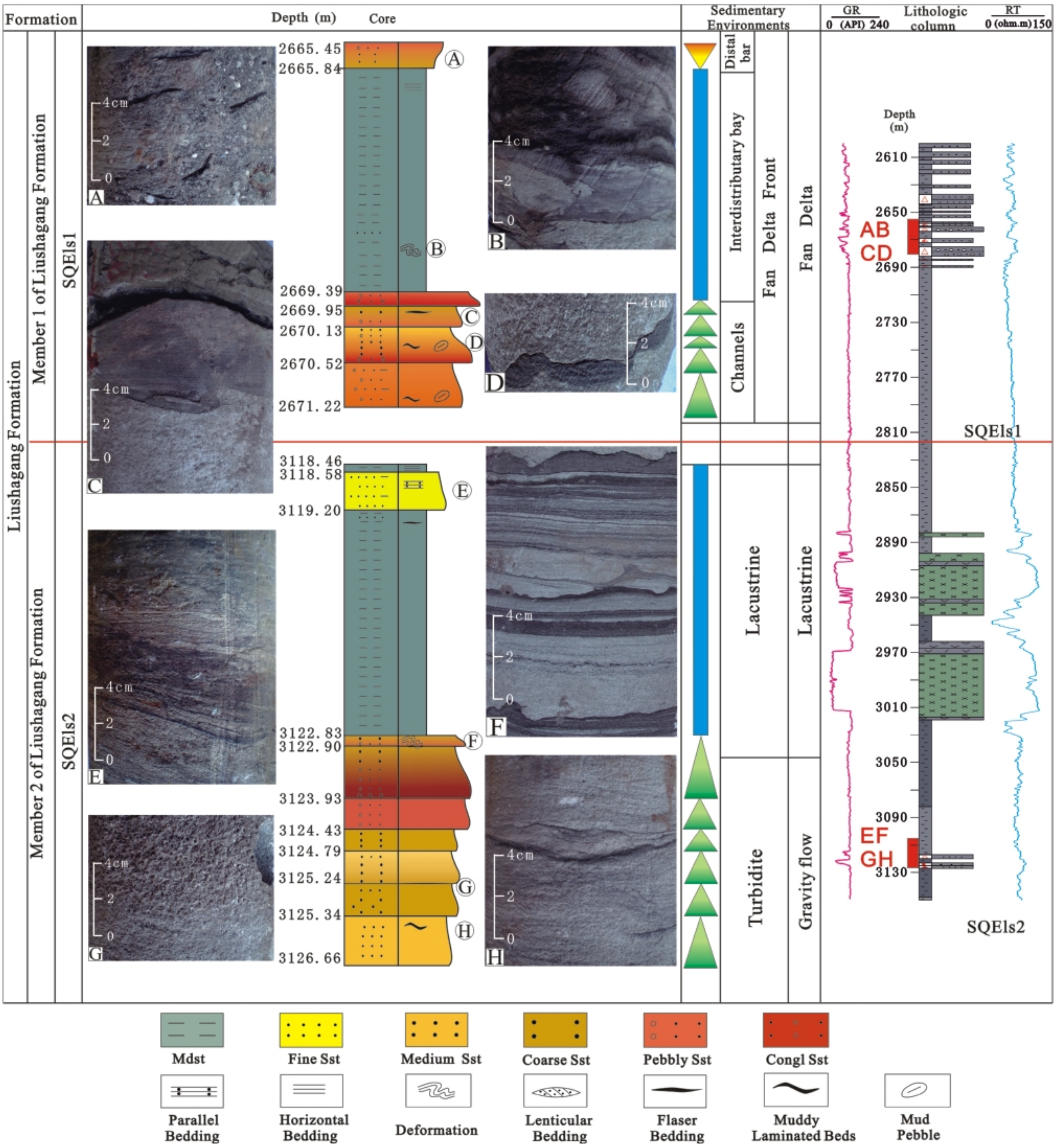

FIGURE 6: Macroscopic view of Well L2 cores. The 13.97 m cores in SQEls2 and SQEls1 occur from 3200 m to 2600 m.

The core section of Els1 consists of two lithofacies associations: the lower part is dominated by grey conglomerate sandstones, coarse sandstones, and medium sandstones, as well as fine sandstones, the fining upward sequences are interpreted to be the channels of a fan delta; the upper part of the core section in Els1 developed several coarsening-upward sequences, and dominated by brownish-black and taupe mudstones, grey siltstones, and fine-medium sandstones which is interpreted as delta lobes at the fan delta front and slope. The GR log curve presents the high frequency serrated features.

4.1.2 Well H114

Description:

Well H114 is at the Huachang transfer zone in the central of the Fushan Sag (Fig. 2a). The 27.68 m of cores of SQEls1 from Well H114 are described below (Fig. 5).

From 2700.50 to 2697.55m cores show grey-black mudstone with laminated silty mudstones and organic content (Fig. 5I). Grey pebbly sandstones with black muddy laminated beds (Fig. 5J) are present. From 2573.90 to 2559.10m cores show fine sandstone, medium-coarse sandstone, pebbly sandstone and well sorted sandy conglomerate (Fig. 5B, C) contains erosion surface (Fig. 5H) at the bottom of some fining-upward cycles. Slumps (Fig. 5K), mud pebbles with diverse shapes (Fig. 5E), flaser bedding (Fig. 5D), weak deformations, black muddy laminated beds (Fig. 5G) and muddy pebble (Fig. 5F) are present.

Depositional environment interpretations:

The Well H114 core shows the SQEls1 sequence. The lithologic column is dominated by sandstone and pebbly sandstone. The upper part of the sections shows a fining-upward sequence, abundant conglomerate sandstones with the erosion surface developed in the bottom. The GR log curve has a high frequency serrated shape, which indicates high-energy channel deposits. It is interpreted to be deposited in the distributary channels within a large braided delta environment. The lower part of the core section in Els1 developed several coarsening-upward sequences, interbedded fine-medium sandstone and mudstone with wavy rippled laminations and several deformations in the sandstones; it is interpreted to be the distal bar at a braided river delta front.

The lithofacies described above in Well H114 core for braided river delta systems obviously differ from the fan delta lithofacies described in Well Fc1 core. The poor sorted conglomerates are only developed at the fan delta plain, relative greater mudstones, fine sandstones, well sorted pebble sandstones and thinly interbedded, small-scale cross bedding, and wave-ripples were observed in the braided river delta deposits. The braided river delta environment of a well sorted pebble sandstone deposition is interpreted as a result of sufficient terrigenous sediment influx from Hainan provenance. We interpret these differences also in view of the braided river delta strata deposited at greater distances from the source area rather than the fan delta strata; the fan delta systems usually located adjacent to the boundary faults. The southern gentle slope in the Fushan Sag with an area of 986km2 (Fig. 2b) is beneficial for long distance transportation of sediments that have provided favorable conditions for the development of braided river delta.

4.1.2 Well L2

Description:

Well L2 is at the Bailian sub-sag in the northeast of the Fushan Sag (Fig. 2a). The 13.97m of cores of SQEls2 and SQEls1 from Well L2 are described below (Fig. 6).

From 3126.66 to 3118.46m cores (SQEls2) show dark grey mudstones intercalated with silt mudstone, grey medium sandstone with homogeneous qualities and conglomerate sandstone, the lower part of cores displaying fining-upward sequences. Laminated bedding, soft deformation of load structure (Fig. 6F) and flaser bedding (Fig. 6H, G) are present. From 2671.22 to 2665.84m cores (SQEls1) show dark grey mudstones, medium sandstone, coarse sandstone and pebbly sandstone, the lower part displaying fining-upward sequences. Muddy laminated beds (Fig. 6C) and mud pebbles (Fig. 6D), parallel bedding and lenticular bedding (Fig. 6B), and imbricated pebbles with mudstone flakes (Fig. 6A) are present.

Depositional environment interpretations:

The Well L2 core shows the SQEls1 and SQEls2 sequence. The lithologic column represents a large set of mudstone of Els2 and the GR log curve has a low frequency serrated shape (ignoring the disturbance of basalt), which is considered to be low energy lake deposits . The cores consists of fine sandstones, and coarse sandstones, as well as pebbly sandstones with deformations and muddy laminated bedding are interpreted to be lacustrine turbidites and deposits of other gravity flow systems.

The core section of Els1 is dominated by conglomerate sandstones, poorly sorted pebble sandstones and fine sandstones, as well as interbedded siltstones and mudstones with several fining-upward sequences that are interpreted to be the channels at the fan delta plain.

4.2 Inter-well correlation, sequence stratigraphy framework and sediment infill features

Identification of sequence boundaries in the Fushan Sag is based on analysis of 3D seismic profiles complemented by well logs and core data. Unconformable stratigraphic contacts denoting sequence boundaries (Fig. 2c and Fig. 7a) are commonly angular unconformities that have strong reflection amplitude and also are represented by abrupt changes in physical characteristics such as lithology and sedimentary facies. Fifty wells with synthetic seismograms, the isochronous sequence stratigraphic framework of the Fushan Sag has been constructed; seven third order sequences comprise the Paleogene section in Fushan Sag which are T2, T3, T4, T5, T6, T7 and

Tg (Fig. 2c and Fig. 7a); six third order sequence boundaries were interpreted which are: SQEch, SQEls3, SQEls2, SQEls1, SQEwz3, SQEwz1+2, as well as three corresponding maximum flooding surfaces within the Liushagang Formation (Els3, Els2 and Els1).

The Inter-well correlation section CC' crosses wells Fc1, H7, Hd4, L15 and Jf6 (Fig. 7b). It is interpreted based on the seismic profile (Fig. 7a), and shows the lithofacies, stratum thickness, and the sediment distribution of the Liushagang Formation. Wells F40 and F24 penetrated SQEls1, wells Fc1 and Y3 penetrated SQEls2, and wells H7, Hd4, L15 and Jf6 drilled through SQEls3 (Fig. 7a). The Fushan Sag represents a graben shape divided by the Huachang transfer zone into a western sub-sag, and an eastern sub-sag.

Western sub-sag: the upper part of the Lingao Fault shows a steep occurrence which resulted in deposition of a coarse clastic steep slope fault belt (Komatsubara, 2004; Feng, 2005; Xu, 2006; Deng et al., 2008). The third Member of Liushagang Formation (Els3) is not developed along the middle and lower part of the Lingao Fault. Due to the proximity to material sources, clast particles within the fans were relatively coarse, and the areal extension of the fans was generally small (Fig. 7b).

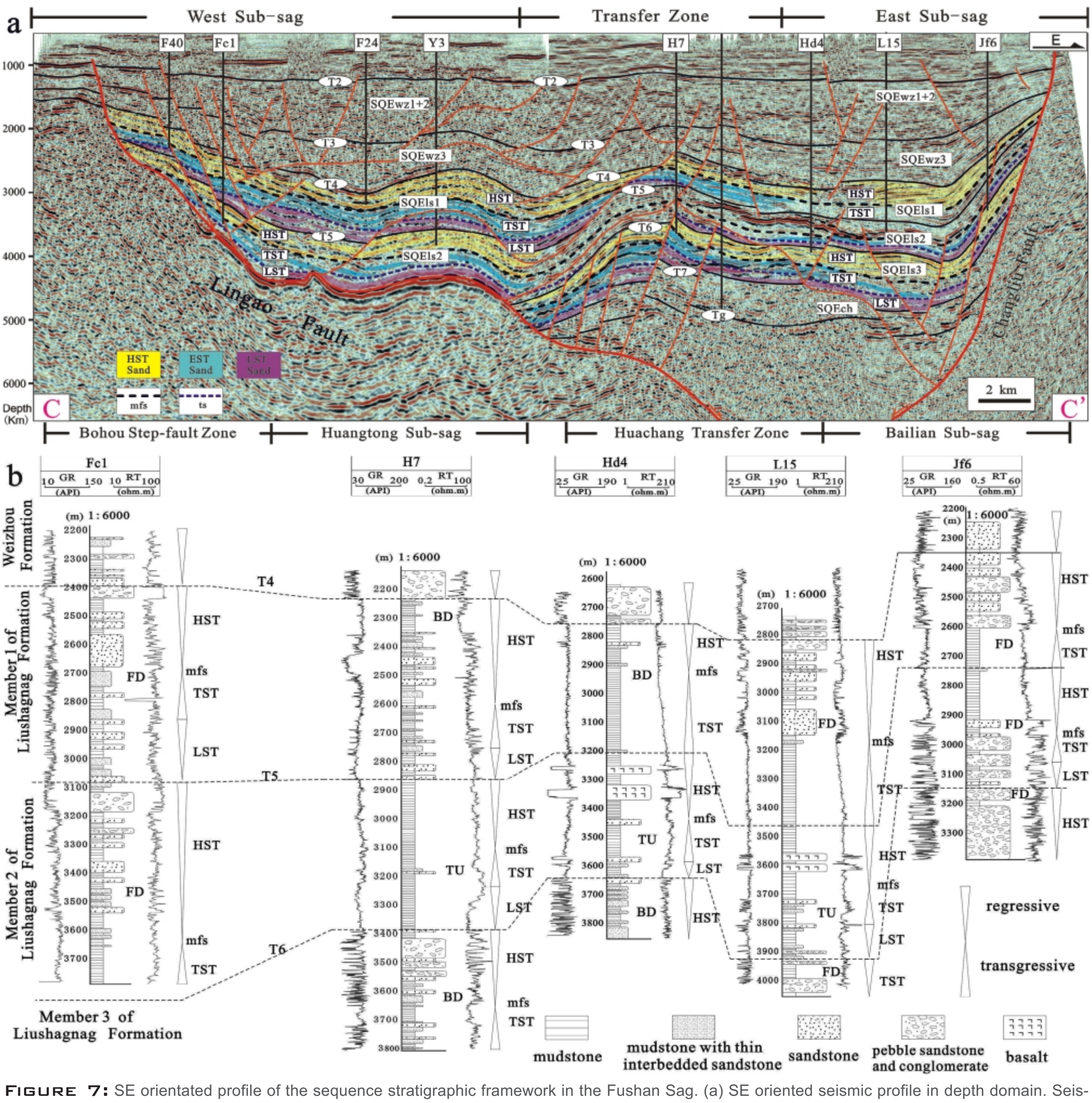

Figure 7: SE orientated profile of the sequence stratigraphic framework in the Fushan Sag. (a) SE oriented seismic profile in depth domain. Seismic reflection of third order sequence boundaries: SQEch, SQEls3, SQEls2, SQEls1, SQEwz3, SQEwz2, SQEwz1. Black dotted lines show the maximum flooding surfaces in the Liushagang Formation. See dotted line CC' in Fig. 2A to locate this survey line. (b) Inter-well correlation section of Well Fc1, H7, Hd4, L15 and Jf6 in the Liushagang Formation. Log curves are natural gamma ray (GR) and true formation resistivity (RT). Abbreviations are as follows: T4, T5, T6= sequence boundary; LST= lowstand systems tract; TST= transgressive systems tract; HST= highstand systems tract; mfs= maximum flooding surface; FD= fan delta; BD= braided river delta; TU=turbidites.

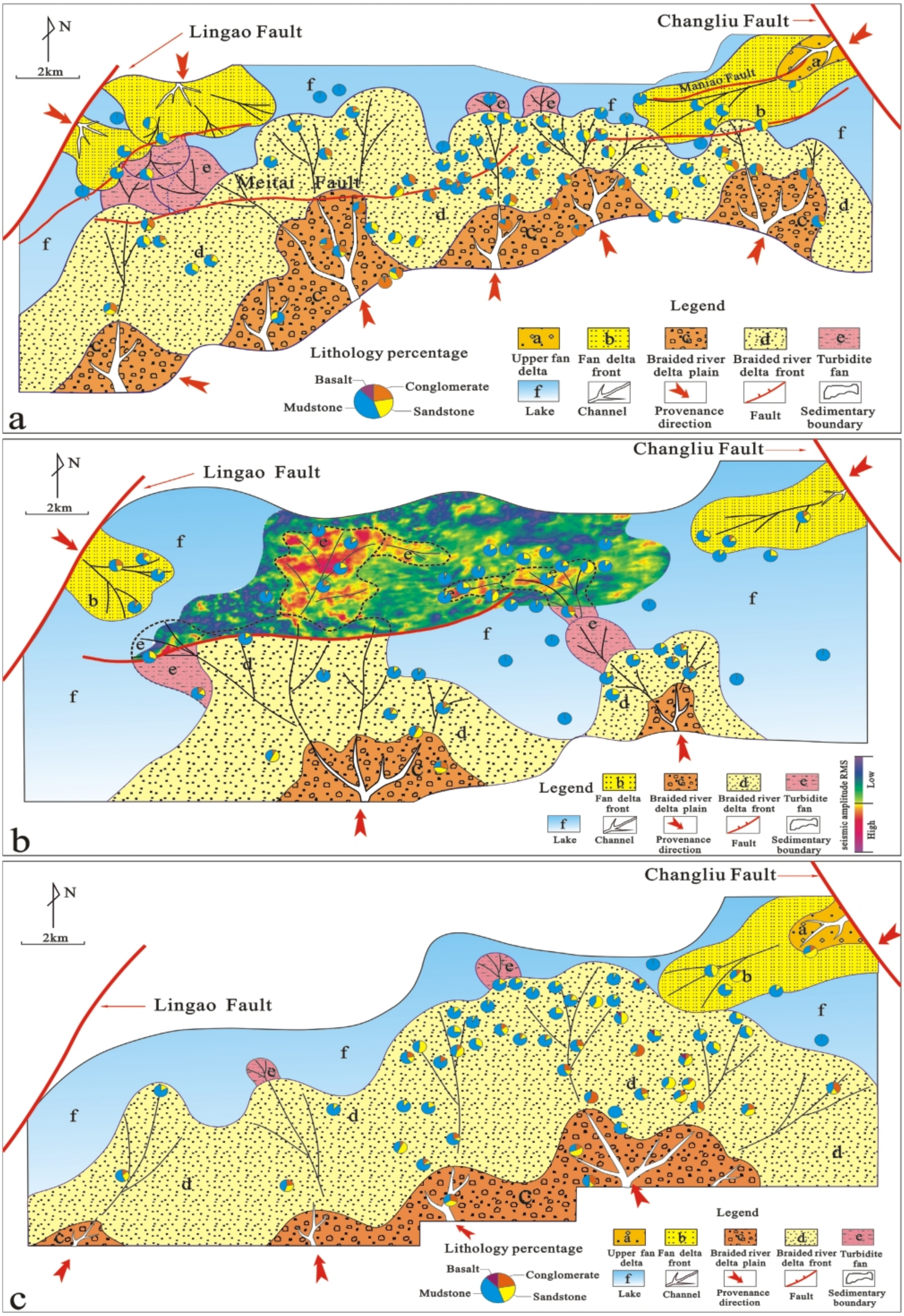
N
2km
Lingao Fault
Changliu Fault
Maniao Fault
Meitai Fault
Lithology percentage
Basalt
Conglomerate
Mudstone
Sandstone
Legend
Upper fan delta
Fan delta front
Braided river delta plain
Braided river delta front
Turbidite fan
Lake
Channel
Provenance direction
Fault
Sedimentary boundary
seismic amplitude RMS
Low
High
a
b
c

Central transfer zone: thick deposits developed in Member 3 of the Liushagang Formation (Els3) that shows a relatively strong sediment input. Member 2 of Liushagang Formation (Els2) is interpreted to be deposited in a lacustrine environment with a generally transgressive trend. During Els1, the sediment input gradually increased, especially at the location of well H7 which developed a large braided river delta with the lateral accumulation.

Eastern sub-sag: due to the proximity to source area of the Yunlong Uplift, it developed a fan delta at wells L15 and Jf6 in Els3 and Els1. The lowstand system tract (LST), the transgressive system tract (TST) and highstand system tract (HST) all represent a fan delta environment during Els3; Els2 is interpreted to be deposited in a lacustrine environment; During Els1, LST is not developed, TST is dominated by a lacustrine sedimentary system, a large scale fan delta deposits with a long progradation is developed in the HST.

4.3 Temporal and spatial evolution of the Liushagang Formation

According to the comprehensive analysis of the core lithology, well drilling, log curves, seismic amplitude data (as shown in Fig. 8b) and sand content statistics (as shown in Fig. 8), the sedimentary distribution of Fushan Sag in the Liushagang Formation were defined. Controlled by boundary faults, three main sources of sediment supply were around the Fushan Sag, forming the northern, northwestern, and northeastern delta systems (See the red arrow in Fig. 8 as the source direction). Depositional systems identified in the Fushan Sag include fan delta (upper fan delta, delta fronts), braided river delta (braided river delta plains, delta fronts), turbidite deposits and lake systems. Similar depositional systems have been recognized in other Paleogene sub-basin in the Beibuwan Basin (Liu, 2009; Wang et al., 2010; Jiang, 2009; Yang et al., 2012). Braided river delta deposits are widely developed in the southern part of the Fushan Sag, whereas fan delta systems are located in northwestern and northeastern basin margin faults of the Fushan Sag. The abundant coarse clastic and poorly sorted sediments in Member 3 of Liushagang Formation (Els3) are interpreted to be a delta deposit. A large set of mudstone and the obviously decreased sandstone percentage in the Member 2 of Liushagang Formation indicate a regional transgressive process during Els2, which mainly developed lacustrine deposits. When the lake level rises, the size of the braided river delta was reduced. As a result of strong activity of the Meitai Fault, turbidite deposition on the hanging wall is developed, and the spatial distribution, sedimentology and strata architecture are under syn-rift control (Li et al., 2010). According to the seismic amplitude analysis (Fig. 8b), the turbidite deposition is also developed in the Huachang transfer zone during Els2. The uplifting of Hainan Basement leads to general subaerial exposure of the southern area during Els1, and the depocenter migrated northward. The braided river delta in the south part developed continuously with a turbidite fan lakeward at the delta front in the Huachang transfer zone, and braided river delta front in the west deposited further distance away from the Meitai Fault towards north.

Figure 8: Lacustrine sedimentary distribution map in Liushagang Formation of the Fushan Sag (a = upper fan delta; b = fan delta front; c = braided river delta plain; d = braided river delta front; e = turbidite; f = lake). (a) SQEls1 sedimentary system distributions. (b) SQEls2 sedimentary system distributions. (c) SQEls3 sedimentary system distributions. The provenances came from the northeastern Fan Delta, the southern Braided River Delta, and the northwestern Fan Delta.

The secondary faults in the sag controlled the distribution of the subfacies. The Meitai Fault with a NEE trending and 28km extended length, is located at the west of the Fushan Sag and was formed by intense extension. It controls the braided river delta plain and front (during Els2 and Els1). The Maniao Fault and other two parallel faults with a NE trending derived from the Changliu Fault by strike slip, which formed a fault accommodation space (James and Robert, 1988; Wang et al., 2011; Jin et al., 2013) that controls the Bailian fan delta in the northeast of the Fushan Sag. Braided river delta as a major sediments influx developed in the central part of the Fushan Sag during Els3 and Els1, which was obviously controlled by the Huachang transfer zone.

5. Discussion

The sediment infill in the Fushan Sag was controlled by the basin evolution during the Paleogene as well as synsedimentary tectonic activity.

5.1 Lingao Fault, Changliu Fault and Meitai Fault activity

The activity of growth faults was calculated based on the fault heave analysis. The boundary faults such as the Lingao Fault and the Changliu Fault were all active during Els3 to Els1, and the Meitai Fault was active since Els2. Along the western boundary, Lingao Fault and Changliu Fault activity initially increased from Els3 to Els2 and then decreased during Els1 (Fig. 9). The development of Meitai Fault started during Els2, and then increased obviously during Els1. In general, the Lingao Fault and Meitai Fault are more active than the eastern boundary Changliu Fault, which has an important influence on the depocenter migration and the development of the western part braided river delta front in Huangtong Subsag. The average activities of Lingao Fault in each period are 27 m/Ma during Els3, 60 m/Ma during Els2, and 35 m/Ma during Els1. The average activities of Meitai Fault in each period are 27 m/Ma during Els2, and 38 m/Ma during Els1. Compared with the Lingao Fault and the Meitai Fault, the Changliu Fault was less active. The average activities of Changliu Fault in each period are 25 m/Ma during Els3, 24m/Ma during Els2, and 9.5 m/Ma during Els1.

5.2 Strata thickness response to the tectonic activities

Sediment thickness reached a maximum of more than 2200 m in total (located at the northern part of the Meitai Fault) during

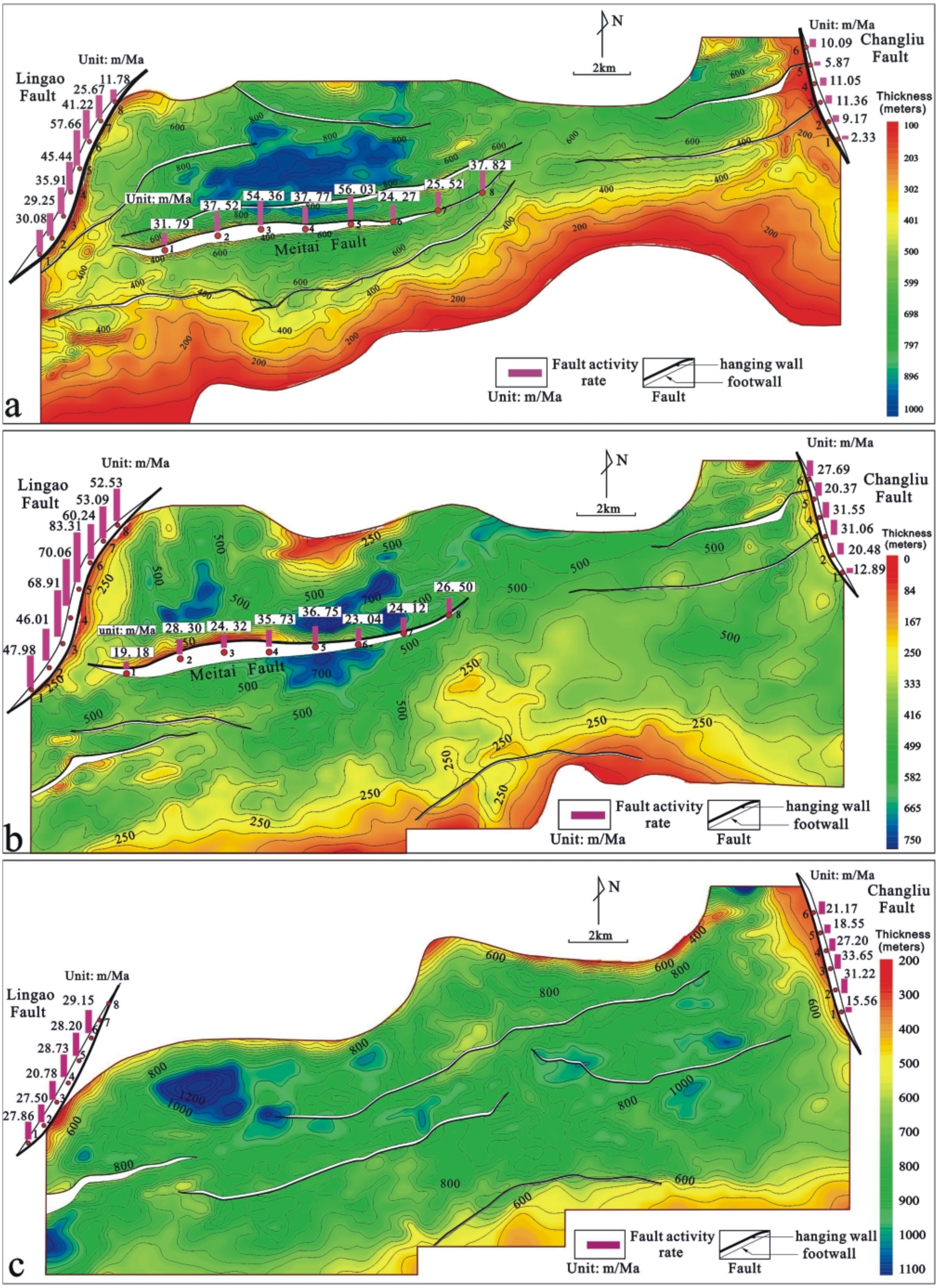

Figure 9: Strata thickness, boundary faults and Meitai Fault activities of the Fushan Sag at different stages in the Liushagang Formation. See purple bar chart in A, B, C to locate those faults. (a) Strata thickness, boundary faults and Meitai Fault activity rate of SQEls1 (b) Strata thickness, boundary faults and Meitai Fault activity rate of SQEls2. (c) Strata thickness and boundary faults activity rate of SQEls3. Thickness unit: Meter; fault activity rate unit: m/Ma.

the Liushagang Formation (Fig. 9). The main depocenter was at the northwestern part of the Fushan Sag with a maximum thickness of 1200 during Els3 (Fig. 9c), and the thickness distributions during Els3 were relatively homogeneous. In the Els2 stage, the sequence thicknesses were reduced to a maximum thickness of 900 m (Fig. 9b). As a result of the Meitai Fault activity during Els2, the northern depocenter became important, and the strata thickness along the southern slope decreased. The main depocenter was at the hanging wall of the Meitai Fault, and the orientation of the depocenter was parallel to the strike of the Meitai Faults. The depocenter migrated eastwards from Els2 to Els1, with a maximum thickness increase from 950 m to 1050 m, parallel to the strike of the Meitai Fault. (Fig. 9a).

5.3 Subsidence history

Typical seismic profiles DD' and EE' were selected in the Fushan Sag (See Fig. 2a for the plan location) for backstripping subsidence history. The sedimentary evolution survey line DD' (Fig. 10a) is located in the western part of the sag; the depocenters were located in the north near the Lingao Fault and pinching out gradually to the south. Both the thicker northern strata and relatively thinner southern strata developed continuously from Els3 to Els1. The sedimentary evolution survey line EE' (Fig. 10b) is located in the eastern part of the sag, where the northern strata are thicker. The constantly increasing area of subsidence indicates that the Fushan Sag widened considerably from Els3 to Els1.

5.4 Geomorphology and sedimentary evolution of the Liushagang Formation

The temporal and spatial interaction of paleotopography, paleolake evolution, synsedimentary faulting and different structural styles, and sequence stratigraphic architecture, controls the development and geometry of the sedimentary systems in the Fushan Sag. A 3D seismic cube requiring time-to-depth conversion and 3D back-stripping were used to reconstruct the paleotopography. In the sequence from SQEls3 to SQEls1 (Fig. 11), the intense fault rifting to overall subsidence is the result of subsidence decreasing in the Paleogene, from the deposition of the Liushagang Formation to the Weizhou Formation. In the early stage, syn-rift fault control is a dominant factor influencing stratigraphic architecture; both the western and eastern sediment sources were controlled by two boundary faults. During Els2 period, tectonically induced uplift and subsidence ceased and became stable. Sedimentation developed continuously, and the size and progradation distance of the delta system gradually declined from SQEls3 to SQEls2 (Fig. 11a, b). This was followed by a transgression leading to increased water depth. The sag size was decreasing and erosion took place, with all kinds of delta sand bodies. This was followed by regression. Lake level rise and high sediment flux characterized the Els1 stage in the Fushan Sag (Fig. 11c).

6. Conclusions

1) Four depositional systems were identified in the Paleocene to Eocene of the Fushan Sag: fan delta sedimentary system (including upper fan delta and delta fronts), braided river delta system (including braided river delta plains and delta fronts), and turbidite deposits in a lake system.
2) During the Eocene, from Els3 to Els2, a lake transgression was recognized by the decreasing sandstone percentage and the changing sedimentary environment. From Els2 to Els1, large-scale delta developed with falling lake level and abundant sediment supply, which shows a regressive process.

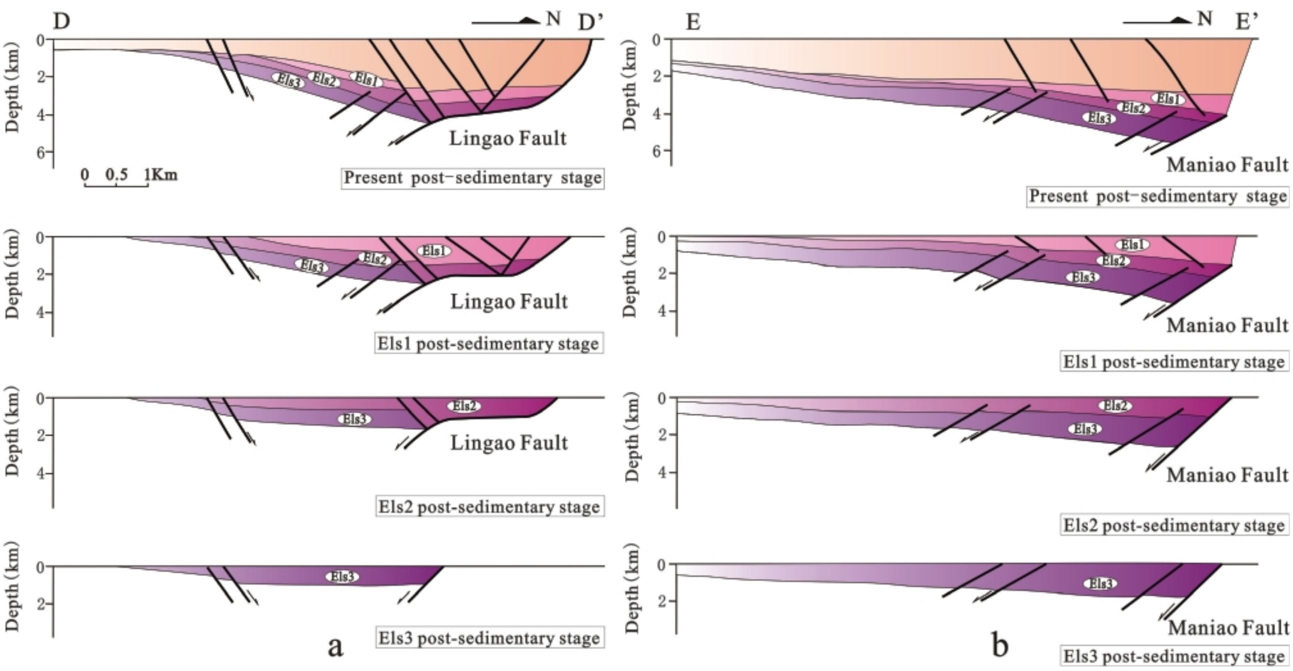

Figure 10: Subsidence history recovery profiles of the Liushagang Formation in the Fushan Sag. Unit: Km. See green lines DD' and EE' in base map to locate this survey line.

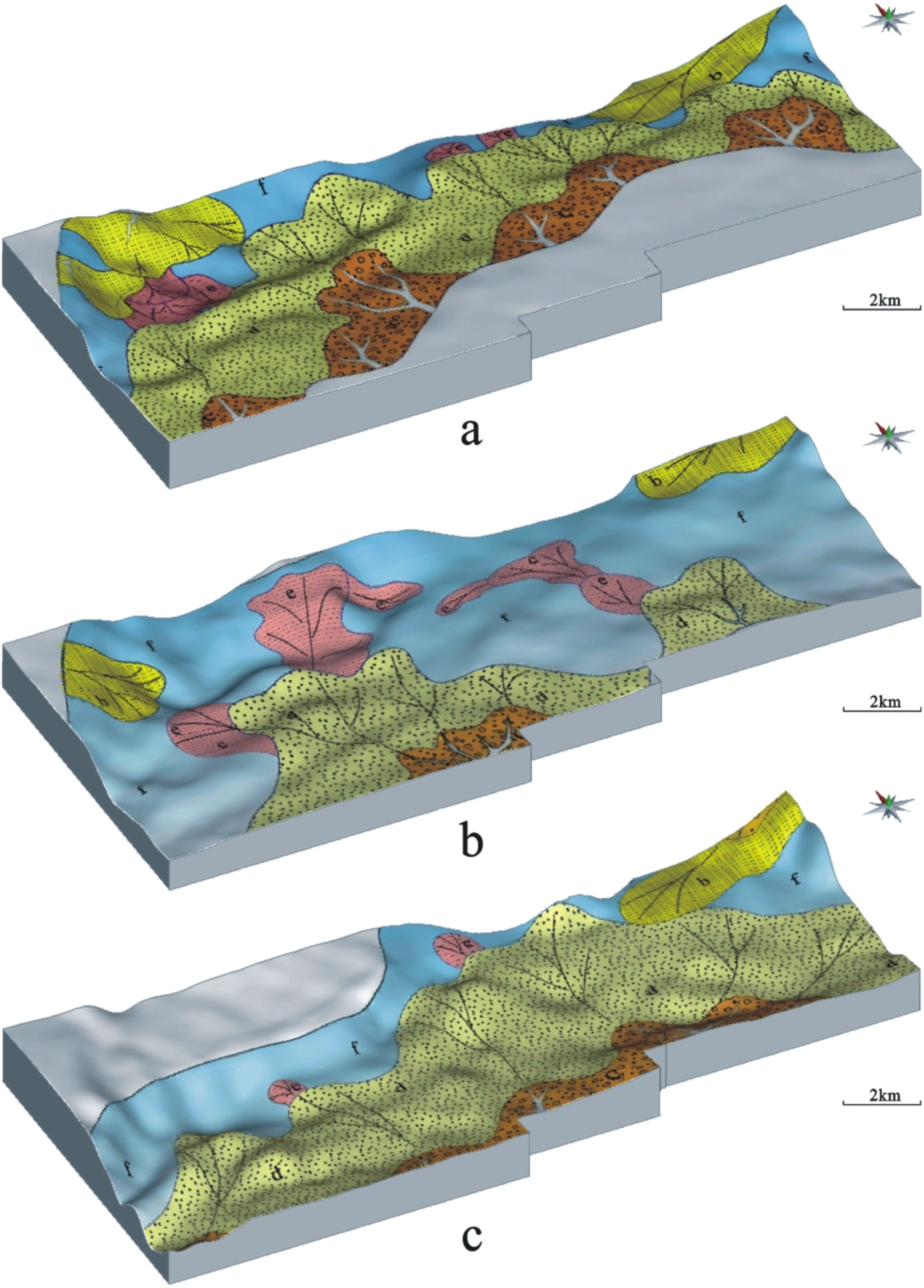

Figure 11: Sketch drawings of the paleotopography and sedimentary system evolution of the Liushagang Formation during the Eocene (See legend in Fig. 8) (a = upper fan delta; b = fan delta front; c = braided river delta plain; d = braided river delta front; e = turbidite; f = lake). (a) SQEls1. (b) SQEls2. (c) SQEls3.

3) The braided delta and two fan deltas developed from Els3 to Els1 with their size decreasing first and then increasing.
4) Syn-depositional tectonics controlled the sediment fill and the location of depocenters. The active boundary faults of the western Lingao Fault and eastern Changliu Fault, where fault activities increased first and then decreased, have a great influence on the shape of the two fan deltas and the migration of depocenters in the Liushagang Formation. The activity of Meitai Fault started during Els2 with an obviously increasing activity which controlled the distribution of braided river delta plain and delta front.
5) The subsidence diminished continuously during the Eocene, from Els3 to Els1, with an inherited topography. This indicates that the dominant geological process varied from intense fault rifting in the Paleocene to early Eocene to relatively gentle and overall subsidence during the middle to late Eocene.

Acknowledgments

This paper benefited from the abundant valuable data provided by the Research Institute Exploration and Development, PetroChina Fushan Oilfield Company. The authors would like to express their sincere gratitude to the National Major Science and Technology Project of China (Grant No. 2011ZX05009-002) and the Open Project Foundation of Key Laboratory of Tectonics and Petroleum Resources, Ministry of Education, China (No. TPR-2013-12) for their financial supports. The author would also appreciate the editor and anonymous reviewers, and W. Schollnberger whose constructive comments and suggestions have been of great help and enhanced the quality of this work.

References

Chang, Q. M. and Su, H. X., 1986. Types and distribution laws of hydrocarbon reservoir in Beibu Gulf Basin. Marine Geology and Quaternary Geology 6, 55-65 (in Chinese, English abstract).

Chen, L., Gan, H. J., Zhu, C. R. and Tian, J. J., 2002. Study on subsidence history of Weixinan Depression in Beibuwan Basin. Journal of Xinjiang Petroleum Institute 14, 12-17 (in Chinese, English abstract).

Chen, S., Wang H., Lv, Z. Y., Gan, H. J. and Jin, S. D., 2013. Sedimentation of the Lower Cretaceous Xiagou Formation and Its Response to Regional Tectonics in the Qingxi Sag, Jiuquan Basin, NW China. Cretaceous Research 47, 72-86.

Chen, S., Wang, H., Zhou, L. H., Huang, C. Y., Ren, P. G., Wang, J.H., Liao, Y.T., Xiang, X.M., Xia, C.Y., 2011. Recognition and depiction of special geologic bodies of Member 3 of Dongying Formation in Littoral Slope Zone, Qikou Sag. Journal of Central South University of Technology 18, 898-908.

Chen, S., Wang, H., Zhou, L. H., Huang, C.Y., Wang, J.H., Ren, P.G., Xiang, X.M., 2012. Sequence thickness and its response to episodic tectonic evolution in Paleogene Qikou Sag, Bohaiwan Basin. Acta Geologica Sinica-English Edition 86, 1077-1092.

Dahlstrom, C., 1969. Balanced cross sections. Canadian Journal of Earth Sciences 6, 743-757.

Deng, H. W., Wang, H. L. and Wang, D. Z., 2001. Control of paleomorphology to stratigraphic sequence in continental rift basins: take lower Tertiary of western slope in Bozhong Depression as an example. Petroleum and Gas Geology 22, 293-303 (in Chinese, English abstract).

Deng, H. W., Guo, J. Y., Wang, R.J. and Xie, X. J., 2008. Tectono-sequence stratigraphic analysis in continental faulted basin. Earth Science Frontiers 15, 1-7 (in Chinese, English abstract).

Devlin, W. J., Rudolph, K. W., Shaw, C. A. and Ehman, K. D., 1993. The effect of tectonic and eustatic cycles on accommodation and sequence-stratigraphic framework in the Upper Cretaceous foreland basin of Southwestern Wyoming. Sequence Stratigraphy and Facies Associations. Special Publication of the International Association of Sedimentologists. Oxford: Blackwell 18, 501-502.

Ding, W. X., Wang, W. J. and Ma, Y. J., 2003. Characteristics of Liushagang Formation petroleum system in Fushan Depression of Beibuwan Basin. Offshore Oil 23, 1-6 (in Chinese, English abstract).

Du, Z. C., 1997. Structural features and the controlling function of sedimentary from Tertiary in Beibuwan Basin, the South China Sea. Journal of Hebei Mining and Civil Engineering Institute 1, 55-59 (in Chinese, English abstract).

Elena, A. K., Lyal, B. H., Jimmy, P. and Gennady, M. I., 2007. Transfer zones and fault reactivation in inverted rift basins: Insights from physical modeling. Tectonophysics 441, 1-26.

Escalona, A. and Mann, P., 2010. Tectonics basin subsidence mechanisms, and paleogeography of the Caribbean-South American plate boundary zone. Marine and Petroleum Geology 28, 31-62.

Feng, Y. L., Zhou, H. M., Li, S. T., Liu, W. H., Dong, Y. X. and Cao, Z. H., 2004. Sequence types and structural characteristics in continental rift-subsidence basins. Geological review 50, 43-49 (in Chinese, English abstract).

Gong, Z. S., 1997. The Major Oil and Gas Fields of China Offshore. Petroleum Industry Press, Beijing, pp. 199–222 (in Chinese).

He, Y. B. and Gao, Z. Z., 2006. Sedimentary facies of the Liushagang Formation of Paleogene in Fushan Sag of Hainan Island. Journal of Palaeogeography 8, 365-376 (in Chinese, English abstract).

Hentz, T. F., 1995. Diagenesis of Ozona Canyon fracture fills: Implications for potential fractured reservoirs in the Ozona gas play, Val Verde Basin, west Texas, in R. L. Martin, ed., In search of new Permian Basin oil and gas fields: Using today's technologies and tomorrow's ideas for exploration, development, and 3-D seismic in a mature basin: West Texas Geological Society Publication 95-98, 69-81.

James, E. F. and Robert, J. V., 1998. The role of accommodation zones and transfer zones in the regional segmentation of extended terranes. Geological Society of America 323, 1-45.

Jiang, H., 2007. The analysis on depositional characteristic and play for petroleum and gas in initial stage of exploration in offshore faulted basin –Exemplified by Weixi survey, Beibuwan Basin. Diploma thesis, China University of Geosciences (Beijing).

Jiang, H. J., 2009. The analysis of the sequence stratigraphy and the favorable reservoir belts of Liushagang Formation in Maichen Depression of Beibu-Gulf Basin. Diploma thesis, China University of Geosciences (Beijing).

Jin, S. D., Wang, H., Chen, S., Gan, H. J., Lv, Z. Y. and Cao, H. Y., 2013. Control of anticline crest zone on depositional system and its geological significance for petroleum in Changshaling, Yinger Sag, Eastern Jiuquan Basin. Journal of Earth Science 24, 947-961.

Kang, X. D., Zhao, W. C., Pan, Z. G., 1994. Study on architecture of sequence stratigraphic framework of Beibuwan Basin. Journal of Earth Science 19, 493-502 (in Chinese, English abstract).

Li, C. R., Zhang, G. C., Liang, J. S., Zhao, Z. G., Xu, J. Y., 2012. Characteristics of fault structure and its control on hydrocarbons in the Beibuwan Basin. Acta Petrolei Sinica 33, 195-203 (in Chinese, English abstract).

Li, M. J, Wang, T. G., Liu, J., Lu, H., Wu, W. Q. and Gao, L. H., 2008. Occurrence and origin of carbon dioxide in the Fushan Depression, Beibuwan Basin, South China Sea. Marine and Petroleum Geology 25, 500-513.

Li, M. J., Wang, T. G., Lu, H., Wu, W. Q., Liu, J. and Gao, L. H., 2007. A discussion on hydrocarbon accumulation dating determined by homogenization temperature and burial history of fluid inclusions—An example from the Fushan depression, Beibuwan Basin. Oil & Gas Geology 28, 151-158 (in Chinese, English abstract).

Li, Y., Liu, J., Ma, Q. L. and Lu, Z. H., 2010. Sedimentary characteristics of gravity flows within the 1st Member of Paleogene Liushagang Formation of Fushan sag. Special oil and gas reservoirs 17, 30-32 (in Chinese, English abstract).

Liao, J. H., Wang, H., Xiao, J., Li, J. L., Yan, D. T., Li, G. L., Xia, C. Y., Li, Y. L. and Ren, G. Y., 2012. Study on episodic rifting and integrated response process of tectonic, sequence stratigraphy and sedimentary filling in Paleogene of Qiongdongnan basin, South China Sea. Journal of Jilin University (Earth Science Edition) 42, 970-983 (in Chinese, English abstract).

Lin, C.S., Kenneth, E., Li, S. T., Wan, Y. X., Ren, J. Y. and Zhang, Y. M., 2001. Sequence architecture, depositional systems, and controls on development of lacustrine basin fills in part of the Erlian basin, northeast China. AAPG Bulletin 85, 2017-2043.

Lin, C. S., Liu, J. Y., Zhang, Z. Y. and Hu, B., 2005. Sequence stratigraphy and tectonic stratigraphic analysis of tectonically active basins: a case study on the Cenozoic-Mesozoic lacustrine basins in China. Earth Science Frontiers 12, 365-374 (in Chinese, English abstract).

Lin, Z. L., 2011. Research on the tectonic characteristics of Paleogene in Fushan Sag, Beibuwan Basin. Diploma thesis, China University of Geosciences (Wuhan).

Liu, G., Jiang, L., 1995. Balanced section technique and seismic data interpretation. Oil Geophysical Prospecting 30, 833-844 (in Chinese, English abstract).

Liu, J., Sun, M. J., Yue, S. F., Ma, L. N. and Fang, S., 2013. Analysis of diagenesis and major controlling factors of reservoir quality of the Liushagang Formation in Huachang-Bailian Area, Fushan Depression ,Beibuwan Basin. Petroleum Geology and Recovery Efficiency 20, 21-29 (in Chinese, English abstract).

Liu, L. J., Mo, S. G. and Tong, Y. M., 2003. A discussion on the Palaeogene sub-lacustrine fan of Fushan depression in Beibuwan Basin, northern South China Sea. Acta Petrologica et Mineralogica 22, 138-142 (in Chinese, English abstract).

Liu, L. J., Tong, Y. M., Ji, Y. L., Kuang, H. W. and Lu, M. G., 2003. Sedimentary characteristics and developing background of the sub-lacustrine fan in the Liushagang Formation of the Fushan Depression, the Beibuwan Basin. Petroleum Geology and Experiment 25, 110-115 (in Chinese, English abstract).

Liu, P., Xia, B., Tang, Z. Q., Wang, X. G., Zhang, Y., 2008. Fluid inclusions in reservoirs of Weixinan Sag, Beibuwan Basin. Petroleum Exploration and Development 35, 164-169 (in Chinese, English abstract).

Liu, Z. F., Zhao, Z. G., Li, J. H., 2009. The sedimentary facies analysis and its significance in Haizhong Sag, Beibuwan Basin, the South China Sea. Offshore Oil 19, 14-18 (in Chinese, English abstract).

Ma, Q. L., Zhao, S. E., Liao, Y. T. and Lin, Z. L., 2012. Sequence architecture s of Paleogene Liushagang Formation and its significance in Fushan sag of the Beibuwan basin. Journal of Earth Science 37, 667-678 (in Chinese, English abstract).

Nummedal, D., Pomar, L., Posamentier, H. W., Pratt, B. R., Sarg, J. F., Shanley, K. W., Steel, R. J., Strasser, A., Tucker, M. E., Winker, C., 2009. Towards the standardization of sequence stratigraphy. Earth Science Reviews 92, 1-33.

Qiu, Z. J., Gong, Z. S., 1999. Oil Exploration in China (vol. 4), Offshore. Geological Publishing House and Petroleum Industry Publishing House, Beijing (in Chinese).

Shi, X. B., Li, H. X., Huang, C. Y., Pu, X. G., Zeng, Q. B., Chen, S. and Ren, P. G., 2010. Study on the geological bodied in the lower part of the first member of the Paleogene Shahejie Formation in the Qibei Sub-sag in the Huanghua Depression. Geotectonica et Metallogenia 34, 536-544 (in Chinese, English abstract).

Shi, X. B., Zhou, D., Zhang, Y. Y., 2000. Northern marginal lithosphere hot -rheological structure of the South China Sea. Chinese Science Bulletin 45, 1660-1665 (in Chinese, English abstract).

Shi, Y. M., Liu, J. Zhang, M. Z., Chen, D. X. and Ma, Q. L., 2007. Experience and understand in oil and gas exploration in Fushan Sag, Hainan Province. South China Journal of Seismology 27, 57-68 (in Chinese, English abstract).

Strecker, U., Steidtmann, J. R. and Smithson, S. B, 1999. A conceptual tectonostratigraphic model for seismic facies migrations on a fluvio-lacustrine in extensional basin. AAPG Bulletin 83, 43-61.

Song, Z. Q., Tan, C. Q. and Wu, S. B., 2000. The quantitative evaluation standard and weight coefficient of Eocene clastic rock reservoir in Fushan Depression. Fault Block Oil & Gas Field 6, 8-13 (in Chinese, English abstract).

Sun, M., Wang, H., Liao, Y. T., Ren, J. F., Zhao, S. E., Liao, J. H. and Song, G. Z., 2013. Analysis on fan-delta sedimentary system and reservoir-forming conditions of the first member of Liushagang Formation in Bailian area of Fushan sag. Journal of Central South University (Science and Technology) 44: 4150-4160.

Tian, Z. Y. and Wang, S. S., 1985. Geological structures and oil and gas sedimentary basins in the China Seas. Acta Petrolei Sinica 6, 1-10 (in Chinese, English abstract).

Wang, J., Cao, Y. C., Liu, Q. M., Li, J. L, Le, Y. X., Fang, Y., 2010. Flux-turbidite distribution for Paleogene Liu-1 interval west delta front, Wei South-west Depression. Oil Geophysical Prospecting 45, 879-884.

Wang, J. H., Chen, H. H., Wang, H., Jiang, T. and Miao, H. B., 2011. Two types of strike-slip and transtensional intrabasinal structures controlling sandbodies in Yitong Graben. Journal of Earth Science 22, 316-325.

Wang, J. H., Wang, H., Chen, H. H., Zhao, Z. X. and Liao, Y. T., 2007. Research on the tectonic evolution of foreland basins and their responses to deposition and stratigraphy-an example from the Lower Cretaceous in Kuqa Depression. Earth Science Frontiers 14, 114-122 (in Chinese, English abstract).

Wang, J. H., Wang, H., Ren, J. Y., Xiao, D. Q. and Pu, X. G., 2010. A great oblique transition zone in the central Huanghua Sag and its significance for petroleum exploratio. Acta Petrolei Sinica 31, 355-359 (in Chinese, English abstract).

Wei, C. G., He, Y. D., Di, C. B. and Wang, Z., 2008. Faulting mechanism in northern depression of the Beibuwan Basin, China. Geotectonica et Metallogenia 32, 28-35 (in Chinese, English abstract).

Williams, G.D., 1993. Tectonics and seismic sequence stratigraphy: an introduction, in G.D. Williams and A. Dobb, eds., Tectonics and seismic sequence stratigraphy: Geological Society Special Publication 71, 1-13.

Wu G. H. And Qi, J. F., 1999. Characteristics and origin of first order transfer zones in Huanghua Baisn. Oil & Gas Geology 22, 125-128 (in Chinese, English abstract).

Xu, C.G., 2006. Genetic types of Paleogene slope break zones and their controls on depositional system in Bohai off shore. China Offshore Oil and Gas 18, 365-371 (in Chinese, English abstract).

Yan, D. P., Tian, C. L., Meng, L. B., Zhang, J. Z. and Zhou, M. F., 2003. Balanced geological section for extensional tectonic basin and its implication: an example from Southern Songliao Basin. Journal of Earth Sciences 28, 275-280 (in Chinese, English abstract).

Yang, Y. Q., Cui, W. P., Cai, J., Xu, M. Y., 2012. Sedimentary facies of the Member 1 of Paleogene Liushagang Formation of WZ Oilfield in Weixinan Sag, Beibuwan Basin. Journal of palaeogeography 14, 607-616 (in Chinese, English abstract).

Yao, B. and Hayes, D. E., 1998. Lithospheric deformation under the effect of an extensional stress field. Geological Society of China and Academia Sinica 41, 517-534.

Yu, J. H., Liao, Y. T., Lin, Z. L., Li, Y. and Wang, M., 2012. Research on temporal diversity of East-West settlement characteristics of Paleogene in Fushan Sag. Petroleum Geology and Recovery Efficiency 19, 34-38 (in Chinese, English abstract).

Yu, J. J., Luo, Q., Zhang, D. J., Lu, Z. H. and Pang, X. Q., 2004. Characteristics of faults in the Fushan Depression of Hainan, the Beibuwan Basin and their controlling roles to hydrocarbon pool-formation. Petroleum Geology and Experiment 26, 242-248(in Chinese, English abstract).

Zhang, J. R., He, J. X., Gong, X. F., Zhang, X. J. and Huang, W., 2012. Petroleum system, oil and gas migration and accumulation in Fushan Depression, Beibuwan Basin of South China Sea. Marine Geology Frontiers 28, 30-37 (in Chinese, English abstract).

Zhu, W. L., Wu, G. X. and Li, M. B., 2004. Palaeolimology and hydrocarbon potential in Beibu Gulf Basin if South China Sea. Oceanologia et Limnologia Sinica 35, 8-14 (in Chinese, English abstract).

Zhu, W. L., Zhang, G. C. and Gao, L., 2008. Geological characteristics and exploration objectives of hydrocarbons in the norther continental margin basin of South China Sea. Acta Petrolei Sinica 29, 1-9 (in Chinese, English abstract).

Received: 14 March 2014
Accepted: 20 November 2014

Siding JIN[1)2)*)], Hua WANG[1)], Haiyang CAO[1)], Si CHEN[1)], Zhengliang LIN[3)], Jianghao YU[4)] & Songqi PAN[5)6)]

[1)] Key Laboratory of Tectonics and Petroleum Resources, China University of Geosciences, Wuhan 430074, China;

[2)] Department of Geodynamics and Sedimentology, University of Vienna, Althanstrasse 14, 1090 Wien, Austria;

[3)] Sinopec Geophysical Research Institute, Nanjing 210014, China;

[4)] Hubei Institute of Geological Survey, Wuhan 430034, China;

[5)] School of Earth and Space Sciences, Peking University, Beijing 100871, China;

[6)] Petro China Research Institute of Petroleum Exploration & Development, Beijing 100083, China;

[*)] Corresponding author, jinsiding@gmail.com